NUMERICAL ANALYSIS OF THE UNSTEADY CAVITATION SHEDDING FLOW AROUND TWISTED HYDROFOIL BASED ON HYBRID FILTER MODEL

by

Desheng ZHANG[a*], Jian CHEN[a], Lei SHI[a], Guangjian ZHANG[a], Weidong SHI [a], and Bart P. M. van ESCH[b]

[a] Research Center of Fluid Machinery Engineering and Technology, Jiangsu University, Zhenjiang, China
[b] Department of Mechanical Engineering, Eindhoven University of Technology, Eindhoven, the Netherlands

Original scientific paper
https://doi.org/10.2298/TSCI1804629Z

Cavitation is a common phenomenon in components of fluid machinery and it may induce material damage and vibration. A more accurate and commercial turbulence model is required to predict cavitation. In this paper, we make a combination of filter-based model (FBM) and density correction method (DCM) to propose a new DCM FBM. Firstly, the new DCM FBM and the homogeneous cavitation model are validated by comparing the simulation result with the experiment of cavitation shedding flow around the Clark-y hydrofoil and the filter size is determined as well. Then, the cavitation pattern cycle and shedding vortex structure of the twist hydrofoil experimented by Delft University of Technology were predicted using the DCM FBM . The predicted 3-D cavitation structures and development cycle of twist hydrofoil as well as the collapsing features show a good qualitative agreement with the high speed photography results. Numerical results show that the improved turbulence model could predict the cloud cavity evolution well, including the cloud cavity generation, shedding and dissipation. It is found that the re-entrant jet induced by the by adverse pressure gradient is the main reason to generate the cloud cavity shedding. The secondary shedding is also observed which is result from the combination of the radially advancing re-entrant jet and side-entrant jet simulated by the DCM FBM turbulence method.

Key words: *cloud cavitation, twist hydrofoil, density correction, turbulence model, numerical simulation*

Introduction

Cavitation occurs in components of fluid machinery, for instance, suction side of axial pump blade, gap between blade tip, and casing and tip of propeller. The pressure fluctuation caused by the periodic generation and collapse of cavitation bubble induce noise and vibration. Therefore, cavitation control is expected to improve the performance and reliability of the hydraulic machinery.

Turbulence models based on Reynolds averaging has been widely used [1, 2] because of the commonality and memory saving. The disadvantages of RANS model is that it over-predict the turbulent viscosity in the rear part of cavity, where compressible two-phase

* Corresponding author, e-mail: zds@ujs.edu.cn

flow dominants, making the fluid too thick for the re-entrant jet to penetrate. A DCM is proposed by Coutier-Delgosha *et al.* [3], which is effect in predicting shedding cavitation [4-6]. To improve the cavitation prediction accuracy, large eddy simulation (LES), direct numerical simulation, and lattice Boltzmann method which can offer convincing time-dependent results are employed to model the unsteady cloud cavitation. Ji *et al.* [7] and Luo *et al.* [8] used LES model coupled with a mass transfer cavitation model to predict unsteady 3-D turbulent cavitation flow around a twist hydrofoil. However, LES requires a very fine mesh, and the computation cost is also very expensive. Furthermore, it is difficult to obtain a grid-independent solution. Until now, LES method limits the industrial application, especially in hydraulic machines.

In recent years, hybrid models provide a solution for the prediction of turbulent eddy viscosity in the cavitation flow. Taking into account the advantages of RANS and LES, Johansen *et al.* [9] proposed a FBM blending the RANS and LES model to calculate the wake flow of the square object, and obtained a higher prediction accuracy. Many validations [10-17] have been conducted to establish a hybrid FBM for the cavitation flows in a square cylinder, a hydrofoil and hollow-jet valve. The results show FMB can better capture the unsteady features of the cavitation flows than the normal RANS models. However, FMB is not effective in the near-wall region. It indicates the two equation model will be covered when the filter size $\Delta \gg$ l. Furthermore, the filter scale in FBM and the maximum density ratio in the cavitation model have the important effects on the numerical results [14, 15].

Inspired by their work, the objective in this paper is to investigate an economical and accurate simulation method to analyze the cavitation shedding flow around a 3-D twisted hydrofoil, which employed the modified FBM turbulence model and homogeneous cavitation model. The unsteady behavior and evolution of the cavitation shedding flow was analyzed by both numerical and experimental results.

Numerical method description and set-up

Governing equations

Highly developed turbulence is one of the important features of cavitation flow in hydraulic machineries. Its interaction with cavitation and the nature of compressibility of cavity contribute to the intricacy of cavitation flow. The FBM was developed on the basis of standard *k-ε* model by Johansen *et al.* [9]. The governing equations are presented:

$$\frac{\partial(\rho k)}{\partial t}+\frac{\partial(\rho u_j k)}{\partial x_j}=\frac{\partial}{\partial x_j}\left[\left(\mu+\frac{\mu_t}{\sigma_k}\right)\frac{\partial k}{\partial x_j}\right]+P_k-\rho\varepsilon \tag{1}$$

$$\frac{\partial(\rho\varepsilon)}{\partial t}+\frac{\partial(\rho u_j \varepsilon)}{\partial x_j}=\frac{\partial}{\partial x_j}\left[\left(\mu+\frac{\mu_t}{\sigma_\varepsilon}\right)\frac{\partial \varepsilon}{\partial x_j}\right]+C_{\varepsilon 1}P_k\frac{\varepsilon}{k}-C_{\varepsilon 2}\rho\frac{\varepsilon^2}{k} \tag{2}$$

$$\mu_t=C_\mu\frac{\rho k^2}{\varepsilon}F \tag{3}$$

in which C_μ = 0.09, F is the filter function determined by the filter size Δ and turbulence length scale $l_{\mathrm{RANS}} = k^{3/2}/\varepsilon$:

$$F=\min\left[1.0, C_3\frac{\Delta}{l_{\mathrm{RANS}}}\right] \tag{4}$$

Reboud *et al.* [11] and Coutier-Delgosha *et al.* [4] proposed a DCM, which is applicable is reducing the turbulent viscosity in the near wall region. As a combination of FBM and DCM, turbulent viscosity in MFBM is presented:

$$\mu_{t-\mathrm{MFBM}} = C_\mu \frac{\rho k^2}{\varepsilon} F \tag{5}$$

where

$$F = \min\left[f(n), C_3 \frac{\Delta}{l_{\mathrm{RANS}}} \right], \qquad f(n) = \frac{\rho_v + (1-\alpha_v)^n (\rho_l - \rho_v)}{\rho_v + (1-\alpha_v)(\rho_l - \rho_v)}$$

Geometry model

In this paper, a 3-D twisted hydrofoil Twist 11 invented by Delft University of Technology is adopted. The experimental results published provide reference for the simulation [12, 13]. The section of Twist 11 is NACA0009, with a chord length c of 0.15 m and span y = 0.3 m.

Simulation set-up and boundary conditions

The real physical domain is calculated as illustrated in fig. 1, in order to save resources and time. Inlet is 2C from the leading edge and the outlet is 4C from the trailing edge of hydrofoil. The distance between the upper wall and bottom is 2C and left wall is 2C from right wall. Inlet velocity is V_∞ = 6.97 m/s and outlet pressure is defined by $\sigma = (p_{\mathrm{out}} - p_v)/(0.5\rho_l V_\infty^2)$. Symmetric boundary condition is set in the mid plane of span and non-slip boundary condition is employed in walls of tunnel and the surface of hydrofoil.

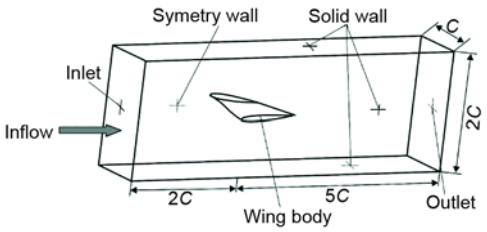

Figure 1. Computational zone and boundary conditions

Convergence evaluation in every step is very important in unsteady cavitation calculation. According to Li [14] and Ji *et al.* [15], excessive iterations in one time step consume too much computation resources, while few iterations induce low precision. So high resolution scheme is used to discrete advection term and second order backward Euler is employed in transient term. Time-step is $\Delta t = T_{\mathrm{ref}}/200 = 1.076 \cdot 10^{-4}$, according to Coutier-Delgosha *et al.* [16], in which $T_{\mathrm{ref}} = c/V_\infty$, and V_∞ is the inlet velocity.

The O-H type structure grid is generated using ANSYS-ICEM, and mesh near wall is refined ($30 \le y^+ \le 100$). With the increase of element number, discrepancy caused by discretion decreases, while error accumulated inclines accordingly. Consequently, it is important to check the grid independence. Three different nodes numbers in span direction are chosen.

As shown in tab. 1, minimum and maximum pressure as well as lift C_{l} and drag coefficients C_{d} predicted by three grids are very close. Grid 2 shows properly the same results with grid 3. So considering numerical precision and resource consumption, Grid 2 is chosen for computation (fig. 2).

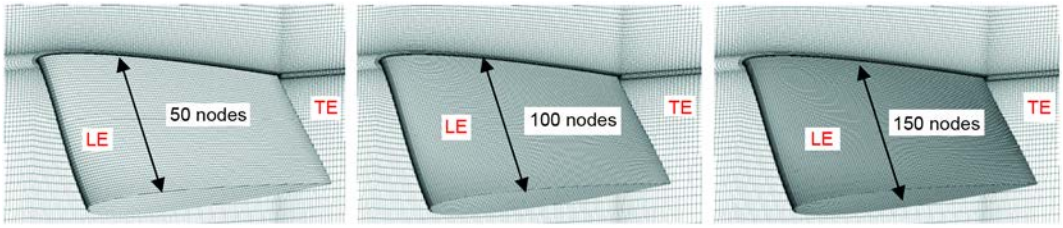

Figure 2. Three cases of mesh around the Delft twisted hydrofoil surface; (a) mesh case 1, (b) mesh case 2, (c) mesh case 3

Table 1. Results of the mesh independence study for twisted hydrofoil

Mesh	Nodes	p_{min}	p_{max}	C_l	C_d
Case 1 (coarse)	1251000	–51941.7	54322.2	0.4643	0.02872
Case 2 (medium)	2502000	–51930.9	54309.2	0.4642	0.02871
Case 3 (fine)	3753000	–51920.6	54346.2	0.4642	0.02871

Results and discussion

Typical cavitation evolution

With the shedding of cavity on the suction surface of twisted hydrofoil, lift force. Time averaged lift coefficient calculated by MFBM is 0.464, which shows a closer result than other reports [7, 18, 19] with the experiment [17], shown as in tab. 2.

Table 2. Time-averaged lift coefficients predicted by various models

	Cal.	Exp.	Error [%]
RANS SST k–ω with correction Li *et al.*, [19]	0.43	0.5167	17
RANS SA with correction Bensow, [18]	0.43		17
Implicit LES Bensow, [18]	0.45		13
PANS Ji *et al.*, [20]	0.453		12
DCM FBM by present	0.464		10

Massive high speed photographs are shot in top view and presented by Foeth [17], one periods of cavitation flow predicted by numerical are compared and depicted in fig. 3, in which cavity is indicated by iso-surface of vapor volume fraction α_v = 0.1. Instants 1~7 marked in fig. 3(a) show cavitation in the one period. Figure 3(b) is the high speed photographs provided by Foeth [17]. Instant 1 shows a convex closure of sheet cavity. As the re-entrant jet driven by adverse pressure gradient enhancing with the inclining adverse pressure gradient, re-entrant jet penetrates into the bottom of cavity and limits the advance of cavity closure downstream. Due to existence of 3-D effect, minor shedding of cavity in area A occurs, which is caused by side-entrant jet. With the re-entrant jet migrates towards the leading edge of hydrofoil, the interface between cavity and liquid start to destabilize. Meanwhile, quasi-steady sheet cavity starts to evolve into highly unsteady cloud cavitation. When re-entrant jet migrates to the leading edge of hydrofoil, main cavity breaks and detaches, as shown in Instant 2 when the total volume of cavity decreases to the minimum. With the main cavity shedding, residual cavity starts to grow and form a concave closure, as illustrated in Instant 3. From In-

stant 4 to Instant 7, shedding main cloud transport downstream and start to roll together. Cavity volume reaches maximum in Instant 5 and with the rolling and breakup of cavity, volume of cavity drops abruptly.

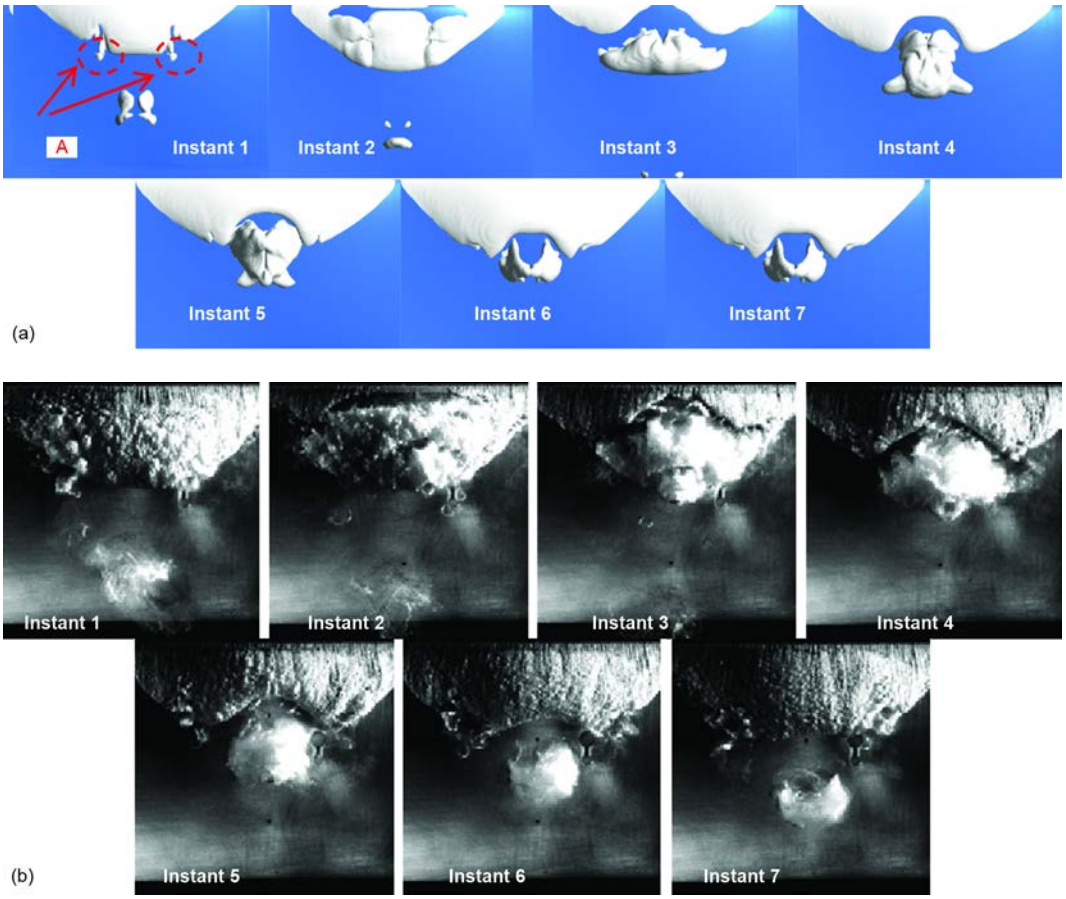

Figure 3. Comparison of observed and predicted cavity volume evolution (σ = 1.07); (a) predicted cavitation evolution in one typical cycle by numerical method, (b) experimental observation of cavitation evolution in one typical cycle (*for color image see journal web site*)

It is reasonable to say that numerical method adopted here well reproduce the cavitation evolution, including the generation, breakup, detachment and collapse of cavity.

Shedding vortex cavitation structure and evolution

In fig. 4(a), the adverse pressure is large enough to drive the re-entrant jet penetrate into the cavity and migrate towards the head of the twisted hydrofoil. In fig. 4(b), a mount of liquid accumulates in the vicinity of hydrofoil head, making a local high pressure region and inducing the breakup of sheet cavity. Corresponding to this instant, cavity volume drops to the minimum. In fig. 4(c), instability of shedding cavity increases, while transport downstream, rolling into highly unsteady cloud cavitation, which is dominant shedding instance in cavita-

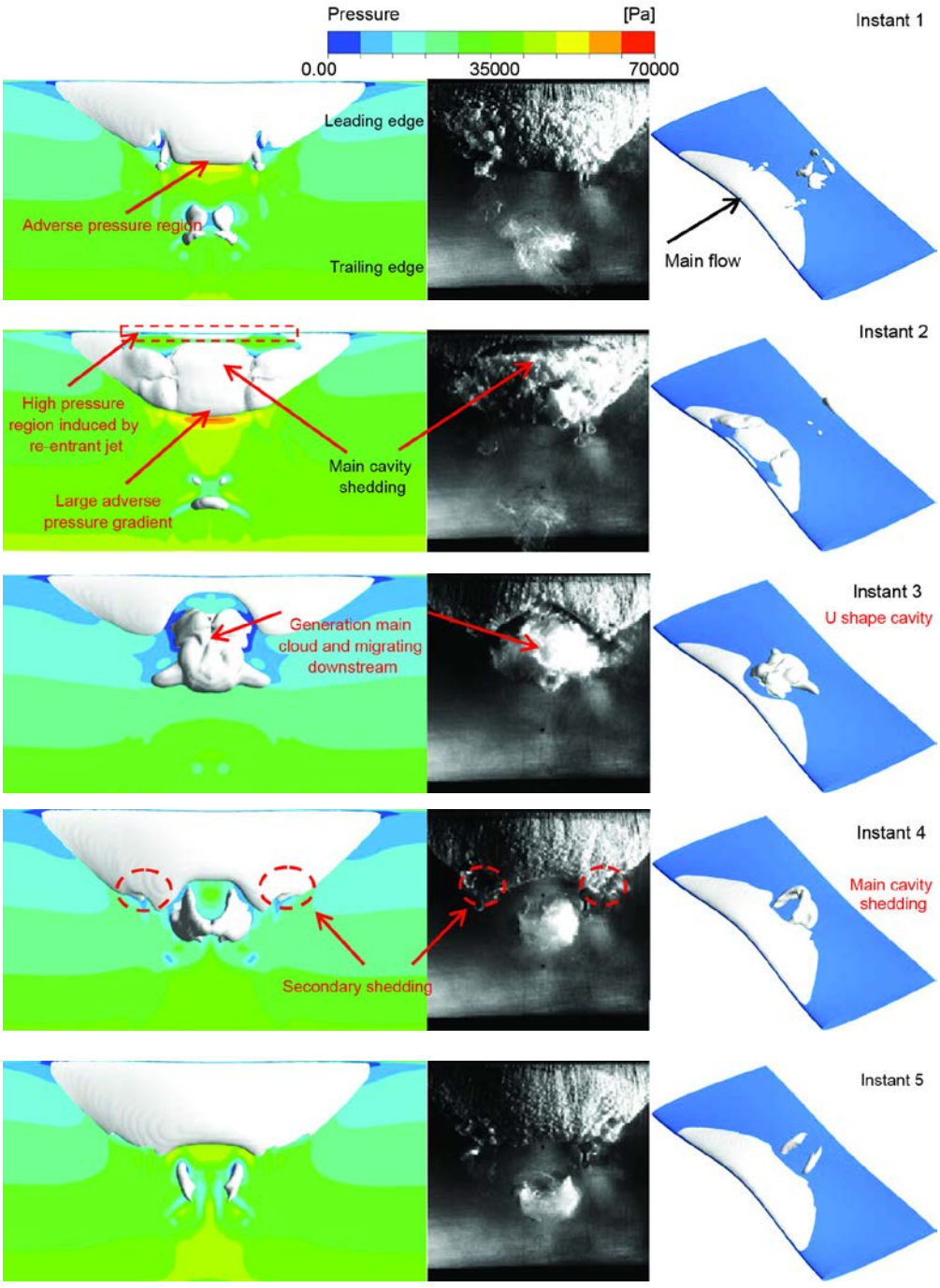

Figure 4. Cavitation patterns during one cavity shedding cycle; numerical top view (left), experimental top view (middle), numerical bird's-eye view (right)
(*for color image see journal web site*)

tion flow field. Cloud cavity becomes more unsteady and transports downstream. Hereafter, generation of sheet cavity slows down and cloud cavitation starts to shrink, as shown in fig. 4(d), and collapses in the high pressure region in fig. 4(e). Figure 4(d) presents the secondary shedding of cavitation near the closure of sheet cavity. Foeth [17] believes that this is caused by the side-entrant jet and we will investigate that on the basis of numerical simulation. Velocity field near the suction side of hydrofoil is depicted in Instant 6 as illustrated in fig. 5. It is distinctive the existence of side-entrant jets on two sides of the attached cavity and the re-entrant jet proceeds radially towards the head of hydrofoil. Re-entrant jet and side-entrant jets collide while advancing and form a liquid band, as indicated in rectangle block in fig. 5. With the liquid accumulating, secondary shedding appears on two sides of sheet cavity.

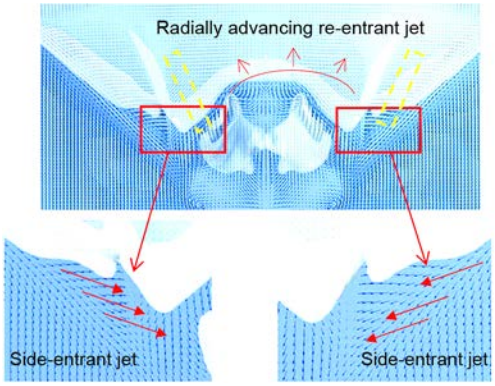

Figure 5. Re-entrant jet and side-entrant jet development at the instant VI
(*for color image see journal web site*)

Based on the previous analysis, it is plausible to say that numerical method adopted in this paper reproduces the pattern and evolution of cavitation around a twisted hydrofoil with precision and accuracy, including the main cloud shedding of main cloud and secondary shedding occurs on both sides of cavity. Specifically, the lobe like cavity and radial side-entrant jet are also predicted in this code. An over-estimation of the collapse of shedding cloud cavity is shown in fig. 4(e), which is consistent with phenomenon predicted by PANS model [20], LES [18, 21] and modified SST k-ω model [19].

Conclusions

- A modified FBM (MFBM) turbulence model is adopted to solve the over-prediction of turbulent viscosity. Combining MFBM with Zwart cavitation model, cavitation flow is simulated and validated. In a macro view, cavitation pattern and evolution show a good agreement with the experiment, which is a good evidence that numerical method employed here is accurate and suitable for cavitation flow simulation.
- Structure and evolution of cavitation on the suction side of a twisted hydrofoil is investigated. Compared with other turbulence, numerical results show that the improved turbulence model could predict the cloud cavity evolution well both in Shedding frequency of cavity and time averaged lift coefficient as well as the process of the cloud cavity generation, shedding and dissipation result from the re-entrant jet.
- The Q-criteria of the vorticity are adopted to study the development of the cloud cavity shedding driven by the high pressure adverse gradient. Both main and secondary cavity shedding are observed by the DCM FBM turbulence model proposed in this paper, and the new method shows more accurate and economical compared to PANS model, LES and modified SST k-ω model.

Acknowledgment

This work was financially supported by the National Natural Science Foundation of China (Grant No. 51776087, 51479083 and 51579118). Transformation of scientific and technological achievements Project of Jiangsu Province (Grant No. BA2016167), Primary

Research & Development Plan of Jiangsu Province (Grant No. BE2015001-3, BE2015146, and BE2016166), 333Project of Jiangsu Province and Six talent peaks project in Jiangsu Province (Grant No. HYGC-008).

References

[1] Launder, B., Sharma, B., Application of the Energy-Dissipation Model of Turbulence to the Calculation of Flow Near a Spinning Disc, *Letters in Heat and Mass Transfer*, *1* (1974), 2, pp. 131-137
[2] Menter, F., *et al*., Ten Years of Industrial Experience with the SST Turbulence Model, Turbulence, *Heat and Mass Transfer*, *4* (2003), 1, pp. 625-632
[3] Coutier-Delgosha, O., *et al*., Simulation of Unsteady Cavitation with a Two-Equation Turbulence Model Including Compressibility Effects*, *Journal of Turbulence*, *3* (2002), 1, pp. 58-65
[4] Coutier-Delgosha, O., *et al*., Numerical Simulation of the Unsteady Behaviour of Cavitating Flows, *International Journal for Numerical Methods in Fluids*, *42* (2003), 5, pp. 527-548
[5] Coutier-Delgosha, O., *et al*., Analysis of Cavitating Flow Structure by Experimental and Numerical Investigations, *Journal of Fluid Mechanics*, *578* (2007), May, pp. 171-222
[6] Leroux, J. B., *et al*., A Joint Experimental and Numerical Study of Mechanisms Associated to Instability of Partial Cavitation on Two-Dimensional Hydrofoil, *Physics of Fluids*, *17* (2005), 5, 052101
[7] Ji, B.,*et al*., Three-Dimensional Large Eddy Simulation and Vorticity Analysis of Unsteady Cavitating Flow around a Twisted Hydrofoil, *Journal of Hydrodynamics*, *Ser. B*, *4* (2013), 25, pp. 510-519
[8] Luo, X., *et al*., Numerical Simulation of Cavity Shedding from a Three-Dimensional Twisted Hydrofoil and Induced Pressure Fluctuation by LES, *Journal of Fluids Engineering*, *4* (2012), 134, 041202
[9] Johansen, S. T., *et al*., Filter-Based Unsteady RANS Computations, *International Journal of Heat and Fluid Flow*, *1* (2004), 25, pp. 10-21
[10] Schumann, U., Subgrid Scale Model for Finite Difference Simulations of Turbulent Flows in Plane Channels and Annuli, *Journal of Computational Physics*, *4* (1975), 18, pp. 376-404
[11] Reboud, J., *et al*., Numerical Simulation of Unsteady Cavitating Flows: Some Applications and Open Problems, *Proceedings*, 5th International Symposium on Cavitation, Osaka, Japan, 2003, pp. 1-10
[12] Foeth, E., *et al.*, Time Resolved PIV and Flow Visualization of 3D Sheet Cavitation, *Experiments in Fluids*, *4* (2006), 40, pp. 503-513
[13] Foeth, E.-J., van Terwisga, T., An Attached Cavity on a Three-Dimensional Hydrofoil, *Procedings*, CAV2006, Wageningen, The Netherlands, 2006
[14] Li, Z., Assessment of Cavitation Erosion with a Multiphase Reynolds-Averaged Navier-Stokes Method, Ph. D. thesis,, Delft University of Technology, Delft, The Nederland, 2012
[15] Ji, B.,*et al*., Unsteady Cavitating Flow around a Hydrofoil Simulated Using the Partially-Averaged Navier-Stokes Model, Chinese *Physics Letters*, *29* (2012), 7, 076401
[16] Coutier-Delgosha, O., *et al.*, Evaluation of the Turbulence Model Influence on the Numerical Simulations of Unsteady Cavitation, *Journal of Fluids Engineering*, *1* (2003), 125, pp. 38-45
[17] Foeth, E. J., The Structure of Three-Dimensional Sheet Cavitation, *Mechanical Maritime & Materials Engineering*, *4* (2008), 24, pp. 125-137
[18] Bensow, R. E., Simulation of the Unsteady Cavitation on the the Delft Twist 11 foil using RANS, DES and LES, *Proceedings*, 2nd Int. Symposium on Marine Propulsors, Hamburg, Germany, 2011
[19] Li, D. Q., *et al*., Towards Numerical Prediction of Unsteady Sheet Cavitation on Hydrofoils, *Journal of Hydrodynamics, Ser. B*, *5* (2010), 22, pp. 741-746
[20] Ji, B., *et al*., Numerical Analysis of Unsteady Cavitating Turbulent Flow and Shedding Horse-Shoe Vortex Structure Around a Twisted Hydrofoil, *Int. Journal of Multiphase Flow*, *51* (2013), May, pp. 33-43
[21] Kubota, A., *et al*., Unsteady Structure Measurement of Cloud Cavitation on a Foil Section Using Conditional Sampling Technique, *Journal of Fluids Engineering*, *2* (1989), 112, pp. 204-210

Paper submitted: January 4, 2017
Paper revised: May 18, 2017
Paper accepted: October 17, 2017